Research Article | Vol. 1, No. 2 | 15 Oct 2018 | OSA CONTINUUM 309
OSA CONTINUUM

Enhancement of modal stability through reduced mode coupling in a few-mode fiber for mode division multiplexing

AAMIR GULISTAN,* SOUVIK GHOSH, AND B. M. A. RAHMAN

School of Mathematics, Computer Science & Engineering, City, University of London, London, EC1V 0HB, UK
*aamir.gulistan@city.ac.uk

Abstract: We demonstrate a novel approach to enhance the modal stability between the modes of a few-mode fiber (FMF) by increasing the effective index differences between these modes. Unlike single mode fibers (SMFs), a FMF guides more than one mode with a larger effective mode area. Mode division multiplexing in FMFs has gained significant importance for potentially high data rate transmission. However, with the increase in the number of modes, a FMF encounters possible coupling between the modes. We proposed two designs of a FMF that supports LP_{01}, LP_{11}, LP_{21} and LP_{02} modes, which propagate with larger mode spacing, offering reduced mode coupling and thus enhancing mode stability. The modal stability or effective index difference between the modes is enhanced by more than 26% by introducing a ring of air-holes in the first fiber design. Moreover, a second fiber design is also proposed, where a five modes fiber is transformed to a four modes fiber and the modal stability enhancement is calculated to be more than 30% without affecting the mode quality significantly. It is also shown here that such a FMF is more resilient to both bending loss and mode area variation compared to a standard SMF. Our proposed technique is scalable and can be used for fibers with a higher number of modes to increase the transmission capacity along with reduced mode coupling.

1. Introduction

Recent studies show that the capacity limitation of a single mode optical fiber (SMF) is rapidly approaching the fundamental Shanon limit [1, 2]. Space division multiplexing (SDM) is considered to be an important approach to overcome the capacity limitation of single core based transmission systems. A multi-core fiber (MCF) or multimode fiber (MMF) has the advantage of boosting the transmission capacity without increasing the fiber count [3]. A few-mode fiber (FMF) has core radius slightly larger than a conventional SMF, which not only enables more guided modes but also results in a larger effective area. This larger effective area of MMF or FMF enhances the power transmission capabilities that may result in longer distance communication and also less sensitive to area reduction due to the external perturbation like bending in fiber [4–6]. However, an important issue arises in FMF transmission system that is the crosstalk or mode coupling between the modes of propagation [7, 8]. The mode division multiplexing in a three-mode fiber using multiple-input multiple-output (MIMO) processing have shown significant transmission capacity improvements over the long distance communication [9]. MIMO based processing techniques are considered necessary to reduce the cross-talk and to reproduce the input signal. However, MIMO introduces latency in the system that further increases with the increased number of modes and also increases the overall complexity of the networks significantly [10, 11]. The cross-coupling between the modes is inversely proportional to the effective index difference between these modes and it is more severe between the neighboring modes. A low effective index difference Δn_{eff} between the modes may result in energy transfer due to inter-mode mixing or energy loss because of the interference between the adjacent modes.

#338696 https://doi.org/10.1364/OSAC.1.000309
Journal © 2018 Received 16 Jul 2018; accepted 13 Aug 2018; published 13 Sep 2018

OSA CONTINUUM

Recently, a high and low index strip doped technique was proposed to increase the effective index difference between the higher order LP_{18}, LP_{09}, LP_{19} modes of a MMF for high power laser transmission systems [12]. Moreover, a MIMO less elliptical core based three-mode fiber design was also proposed to suppress the inter-modal coupling by increasing the effective index difference between LP_{01}, LP_{11a} and LP_{11b} modes [13]. Alexander and Michalis proposed a four-mode fiber with asymmetric refractive index profile that focuses on the enhancement of mode spacing between the LP_{21} and LP_{02}. This resulted in a significant increase in mode spacing between LP_{21} and LP_{02}, however, the initial mode spacing between the LP_{01}, LP_{11} and LP_{21} modes was noticeably reduced [14].

In order to increase the effective index difference (Δn_{eff}) between the modes, we have proposed an innovative approach by introducing an array of air-holes in a FMF. In this paper, we have proposed two FMF designs that supports four guided LP_{01}, LP_{11}, LP_{21} and LP_{02} modes. We have shown significant improvement in the Δn_{eff} and the effect of any possible fabrication tolerances are also discussed. With the higher Δn_{eff}, the difference between propagation constants of the adjacent optical modes becomes larger and the possibility of mode mixing is thus reduced, resulting in improved modal stability. Furthermore, we have also shown that the proposed FMF designs are less susceptible to the bending loss compared to a standard SMF. The numerical simulations are performed using commercially available FEM-based COMSOL software. The proposed fiber design can be fabricated by adopting the similar process that of a Photonic crystal fiber (PCF) with nanometer size air-holes [15, 16].

2. Design strategy to increase the mode spacing in few-mode fibers

First, a four-mode fiber design is considered with a core radius of 7.5 μm and cladding radius of 62.5 μm. The proposed FMF has a Germanium-doped Silica core and Silica cladding with refractive indices of $n_{core} = 1.450$ and $n_{clad} = 1.4403$, respectively. These fiber parameters are considered such that the FMF can allow only four guided modes. The V number using Eq. (1) is calculated as 5.1, where, a is the core radius and λ is the operating wavelength, taken here as 1.55 μm. The V number of 5.1 ensures robustness, good separation between the four modes and cutting off the next higher order modes [17].

$$V = \frac{2\pi a}{\lambda}\sqrt{n_{core}^2 - n_{clad}^2} \tag{1}$$

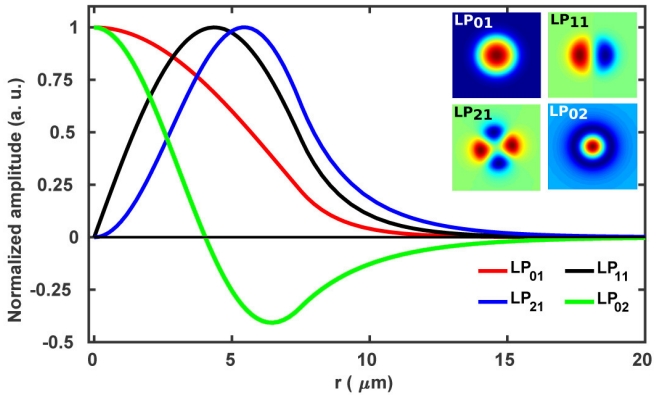

Fig. 1. Normalized H_y field variation of LP_{01}, LP_{11}, LP_{21} and LP_{02} modes along the radius of a step index few-mode fiber, contour field profiles are also shown as insets.

This fiber supports only four guided modes as expected and Fig. 1 shows the normalized

OSA CONTINUUM

dominant H_y field variation of these four LP_{01}, LP_{11}, LP_{21} and LP_{02} modes along the radial axis. For an accurate modal solution, the existing symmetry conditions of the fiber are exploited and only quarter of the structure is simulated [18]. The complete H_y field contours of these modes are also shown as insets in Fig. 1. It can be observed that the field profiles of LP_{01} and LP_{02} shown by red and green lines, respectively, has a maximum amplitude at the center ($r = 0$) of the fiber core. While, the LP_{11} and LP_{21} modes have zero amplitude at the center of the fiber core with peak amplitudes at 5.0 μm and 5.2 μm away from the center, respectively.

The initial mode spacing or effective index differences (Δn_{eff}) between the modes are calculated as $S_1 = \Delta n_{eff}(LP_{01} - LP_{11}) = 2.253 \times 10^{-3}$, $S_2 = \Delta n_{eff}(LP_{11} - LP_{21}) = 2.850 \times 10^{-3}$ and $S_3 = \Delta n_{eff}(LP_{21} - LP_{02}) = 0.821 \times 10^{-3}$. It can be observed that Δn_{eff} between LP_{21} and LP_{02} modes is nearly 3.5 times smaller than the Δn_{eff} between LP_{11} and LP_{21} modes. This very low effective index difference makes these modes highly prone to mode coupling compared with the other modes with a larger effective index difference.

From Fig. 1, it can be observed that the normalized fields of all four modes beyond the core-clad interface decay exponentially. In order to increase the Δn_{eff} between these modes, we have proposed an array of air-holes along the circumference at a particular distance from the core center. The location of air-holes array is directly related to the relative amplitude of these modes. For instance, the normalized amplitudes of the LP_{01}, LP_{11}, LP_{21} and LP_{02} modes at $r = 7.4$ μm are calculated as 0.235, 0.496, 0.664 and -0.344, respectively. Here, at location $r = 7.4$ μm, any positive or negative change in the refractive index would increase or decrease the effective index of these modes, however, magnitude of change would depend on their relative field values at this location. Figure 2 shows the schematic view of a quarter structure of a FMF with the introduction

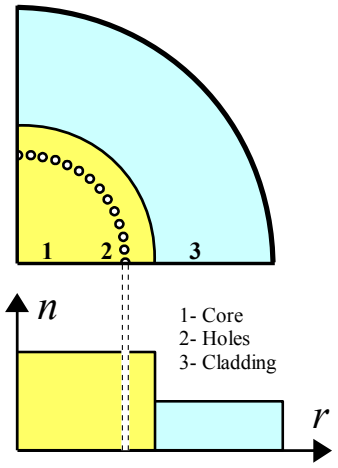

Fig. 2. A schematic illustration showing air-holes in FMF and change in the refractive index profile along the radius of fiber.

of air-holes array. The refractive index change along the radius of fiber is also shown in Fig. 2.

Figure 3(a) shows that the Δn_{eff} between four modes increases with the increase in the size of 200 air-holes introduced at $r = 7.4$ μm from the center of the fiber. For better understanding, the percentage increase in the Δn_{eff} is also calculated with the change in the air-holes size and shown in Fig. 3(b). Here, percentage increase in the stability related to the increase in the effective index difference is calculated by using in Eq. (2)

$$\%\ Stability = \frac{(\Delta n_{eff})_{with\ holes} - (\Delta n_{eff})_{without\ holes}}{(\Delta n_{eff})_{without\ holes}} * 100 \tag{2}$$

It can be noted that with the increase in the size of air-holes, the Δn_{eff} increases nearly linearly.

OSA CONTINUUM

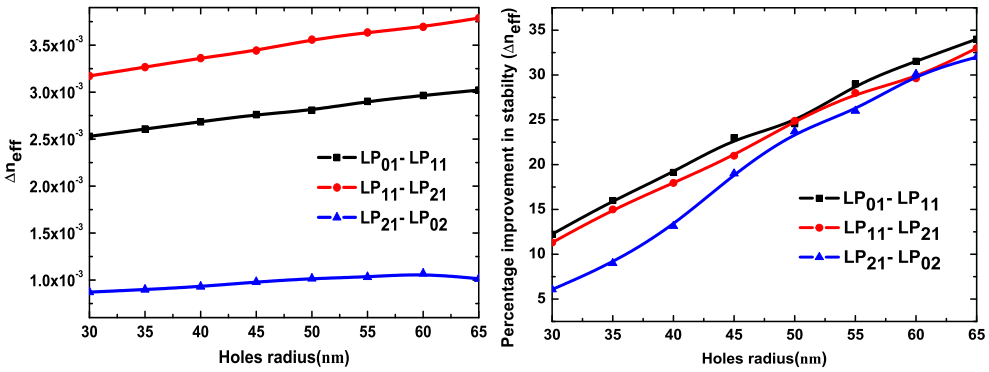

(a) (b)

Fig. 3. Effect on the (a) Δn_{eff} and (b) percentage Δn_{eff} with a change in the hole's radius at $r = 7.4\ \mu m$ along the fiber radius.

This is due to the fact that following introduction of the air-hole array, the effective indices of these modes decrease unequally depending on the relative amplitude of the field at $r = 7.4\ \mu m$.

The modal stability improvement between the modes is observed to be around 26 %, when 200 air-holes each having 55 nm radius are introduced at $r = 7.4\ \mu m$ along the circumference of fiber. However, with the hole radius greater than 60 nm, the LP_{02} mode approaches its cutoff, resulting in the reduction in stability improvement for $\Delta n_{eff}(LP_{21} - LP_{02})$. In case, a three-mode fiber design may be considered, the modal stabilities between first three modes can be increased even more by increasing the radius of air-holes or increasing the number of holes. Moreover, in order to obtain similar Δn_{eff} one can also increase the air-holes diameter while reducing the number of air-holes in array such that the resultant air-holes area remain same.

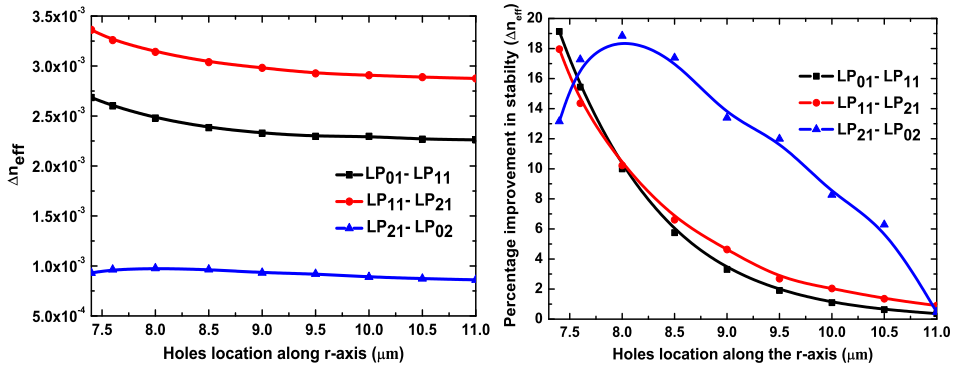

(a) (b)

Fig. 4. Effect on the (a) Δn_{eff} and (b) percentage Δn_{eff} with the change in the hole's array location along the radius of fiber. An array of two hundred air-holes with fixed radius of 40 nm is considered.

In order to select optimum position ($r = 7.4\ \mu m$ in the above case) we have introduced an array of the same number of holes with fixed radius but at the different locations along the fiber radii. Figure 4(a) shows that the modal stability improvement of the modes depends on the location of the introduced air-holes. It is observed that when hole's array is introduced near the boundary

OSA CONTINUUM

of core and cladding, the modal stability enhancement between four modes increases nearly equal. As the air hole's locations is moved from 11 μm to 7.5 μm, the Δn_{eff} values increases continuously, except $\Delta n_{eff}(LP_{21} - LP_{02})$, which shows a saturation. This is due to LP_{02} mode approaching to cutoff and its effective index change becomes small.

The percentage stability improvement for this study is shown in the Fig. 4(b). Here, two hundred air-holes with a fix radius of 40 *nm* are introduced at different locations along the radii of this four-mode fiber. The modal stability improvement increases as the holes array is moved from the $r = 11.0$ μm towards the core radius $r = 7.5$ μm. The percentage improvement in the modal stabilities $S_1 = 15\%$, $S_2 = 14\%$, $S_3 = 17\%$ can be noted when the hole's having radius of 40 *nm* are introduced at 7.6 μm. Here, the location and radius of the air-holes are optimized such that the percentage increase between the four modes remains similar. However, in order to achieve a different percentage improvement or to increase the Δn_{eff} between particular modes similar method can be adopted.

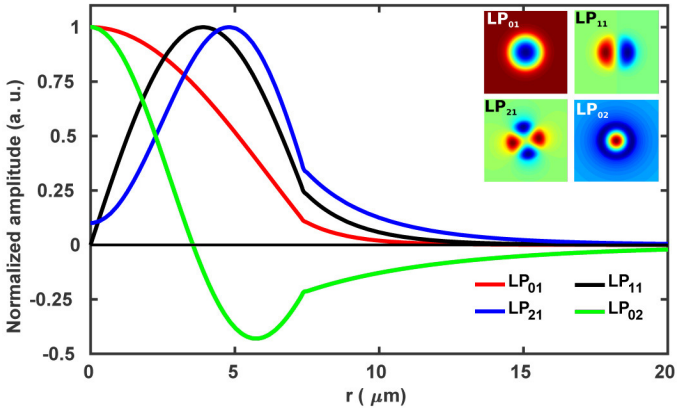

Fig. 5. Normalized H_y fields variations of LP_{01}, LP_{11}, LP_{21} and LP_{02} modes along the radius of modified four-mode fiber, field profile contours are also given as insets.

The introduction of air-hole ring also slightly changes the field profiles of these modes as shown in Fig. 5. The contour field profiles of four modes are also shown as insets. This small field change can be observed at $r = 7.4$ μm along the radius of fiber when an array of two hundred air-holes each having radius of 40 *nm* is inserted in the fiber. The introduction of air-holes affects the magnitude of the field profiles and the normalized amplitude of LP_{01}, LP_{11}, LP_{21} and LP_{02} modes at $r = 7.4$ μm is calculated as 0.107, 0.243, 0.338 and -0.216, respectively. The resultant mode spacings between these modes are calculated as $S_1 = 2.6851 \times 10^{-3}$, $S_2 = 3.362061 \times 10^{-3}$, $S_3 = 0.93006 \times 10^{-3}$ and these represent 19%, 18% and 13% increase, respectively. Additionally, an even higher percentage increase in the effective index difference can achieved when radius of holes is increased.

Figure 6 shows the changes in the effective mode areas of the first four modes with the change in the hole radius. Equation (3) is used to calculate the effective area optical modes of FMF [19].

$$A_{eff} = \frac{[\int |\vec{E}|^2 dxdy]^2}{\int |\vec{E}|^4 dxdy} \tag{3}$$

Here, $\vec{E}$ is the electric field of optical modes and without any air-holes the effective areas of the LP_{01}, LP_{11}, LP_{21} and LP_{02} modes are calculated as 124 μm^2, 177 μm^2, 199 μm^2 and 127 μm^2, respectively. However, the introduction of air-holes reduces the optical field near the air-holes

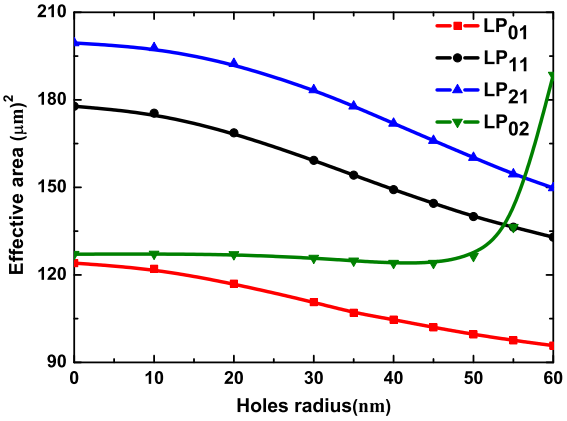

Fig. 6. Effect on the effective mode areas of a change in the hole's size introduced at $r = 7.4$ μm along the radius of modified few-mode fiber.

due to the presence of low refractive index ($n_{air} = 1$) resulting in the reduction of effective mode area. However, it can be noted that the reduction of the mode area is less than the modal stability enhancement.

The introduction of air-holes also reduces the field intensity beyond the location of air-holes array. With the fixed number of air-holes at $r = 7.4$ μm, the effective area of the first three modes continue to decrease but the effective area of LP_{02} increases when the air-hole size is increased more than 55 nm as this mode approaches its cutoff. However, with the small decrease in the effective area of these modes the resultant modal stability improvement of more than 26% is achieved and this can be increased further between the first three modes. The resultant effective areas of first three LP_{01}, LP_{11} and LP_{21} modes are calculated as 95.7 μm^2, 132.9 μm^2, and 149.7 μm^2, respectively. Moreover, as the LP_{02} mode approaches to cutoff condition for air-hole size of 60 nm and its effective area is increased to 188.49 μm^2. Reduced mode area may limit the power handling capability but these mode area values are still significantly larger than the SMFs along with increased mode separation which will reduce mode coupling appreciably.

3. Reduction of five modes to four modes for improved mode spacing

For the four-mode fiber design presented above, although it would have been possible to enhance further the Δn_{eff} between the first three modes, however, the $\Delta n_{eff}(LP_{21} - LP_{02})$ reaches to its saturation. In case we would like to enhance the Δn_{eff} between all the four modes further, a fiber which can guide five modes can be considered. In order to achieve higher mode effective index difference, next a fiber with a larger core size is considered which can guide five modes. The core radius for the second fiber design is increased from 7.5 μm to 8.5 μm whilst keeping the core and cladding refractive indices same as the first fiber.

The V number for the second fiber is calculated as 5.77 at the same operating wavelength of 1.55 μm. This fiber guides five, LP_{01}, LP_{11}, LP_{21}, LP_{02} and LP_{31} modes. The Δn_{eff} between these modes are calculated as $\Delta n_{eff}(LP_{01} - LP_{11}) = 1.842 \times 10^{-3}$, $\Delta n_{eff}(LP_{11} - LP_{21}) = 2.360 \times 10^{-3}$, $\Delta n_{eff}(LP_{21} - LP_{02}) = 0.7396 \times 10^{-3}$, $\Delta n_{eff}(LP_{02} - LP_{31}) = 2.050 \times 10^{-3}$.

In order to increase the effective index difference between the first four modes an array of two hundred air-holes ($r_{air} = 50$ nm) is introduced at different locations along the radii of the second fiber. Figure 7 shows the percentage increase in the modal stability between the first four modes as the air-hole array reaches to the core. The stability improvements between all four modes have similar increase near the core and cladding interface. However, when air-hole's array is moved further inside the core the stability between first three modes keep on increasing

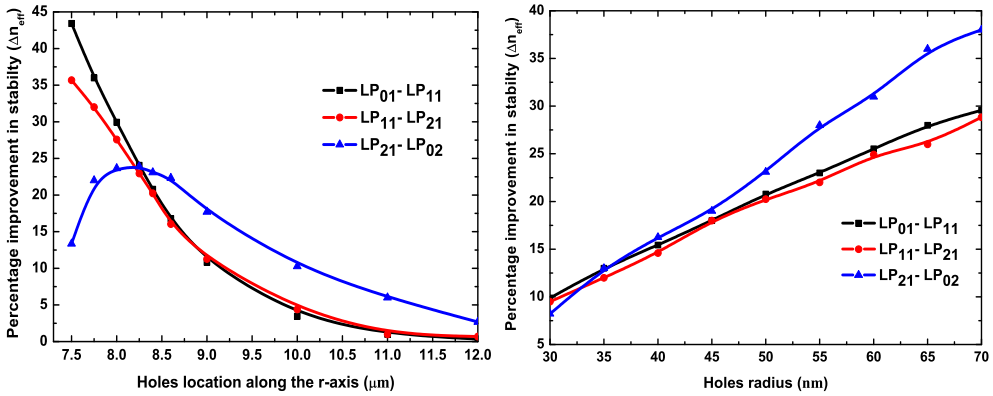

(a) (b)

Fig. 7. Effect on the percentage stability improvement of a change in the (a) location of hole's array along the radius (hole radius=50 *nm*) (b) hole's size introduced at $r = 8.4\ \mu m$ for the second fiber design.

but the fourth LP_{02} mode approaches to cutoff when $r < 8.0\ \mu m$. Similarly, as the array of air-hole is moved away from the core and towards cladding the modal stability improvement reduces as a linearly fashion. The increase in the effective index differences S_1, S_2 and S_3 is calculated as 2.225428×10^{-3}, 2.838742×10^{-3}, 0.91042×10^{-3}, respectively, for the second fiber when the two hundred air-holes each having 50 *nm* radius are introduced at a distance 8.4 μm from the center. The resulting percentage increases are calculated as $S_1 = 21\%$, $S_2 = 20\%$ and $S_3 = 23\%$ as shown in Fig. 7(a). Moreover, percentage improvement in the Δn_{eff} between four modes improves with the increase in air-hole radius as shown in Fig. 7(b). As the air-holes size is increased the effective indices of these modes decreases depending on their relative field amplitudes near the air-holes. When the air-holes radius is increased to 70 *nm*, the modal stabilities S_1, S_2 and S_3 are calculated as 2.387×10^{-3}, 3.041×10^{-3} and 1.02×10^{-3}, respectively. Corresponding percentage increase are noted as $S_1 = 30\%$, $S_2 = 29\%$ and $S_3 = 38\%$.

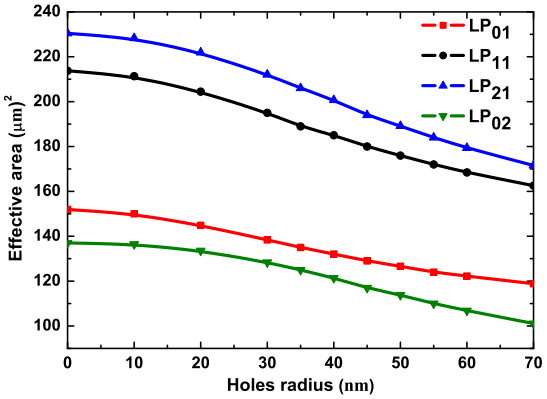

Fig. 8. Effect on the effective mode areas of a change in the hole's size at $r = 8.4\ \mu m$ along the radius of second fiber design.

The effective area of first four modes in the second fiber design also increases due to larger core size compared to the first fiber design. The effective areas of LP_{01}, LP_{11}, LP_{21} and LP_{02}

OSA CONTINUUM

modes are calculated as 151.92 μm^2, 213.77 μm^2, 230.45 μm^2 and 137.00 μm^2 for the second fiber design, respectively. Figure 8 shows the effect on the effective area of first four modes as the air-holes size is increased. It can be observed that as the air-holes size is increased the effective areas of the modes reduces. When the radius of air-holes is increased to 70 nm the resultant effective area of LP_{01}, LP_{11}, LP_{21} and LP_{02} modes are calculated as 118.85 μm^2, 162.55 μm^2, 171.57 μm^2 and 101.09 μm^2, respectively. Table 1 summarizes the effective index differences between LP_{01}, LP_{11}, LP_{21} and LP_{02} modes and effective areas when 200 air-holes are introduced in our proposed designs.

For a four mode fiber, the LP_{02} mode is closer to cutoff value (refractive index of cladding) as compared to five mode fiber design where the LP_{31} mode is near to the cutoff value. Hence, adding air-holes in a four modes fiber the effective area of LP_{02} mode start increasing due to reaching its cutoff as shown in Fig. 6. On the other hand, for a five mode fiber, the effective area of LP_{02} mode shows a linear decrease as being further away from the cutoff and does not approach to cutoff value as shown in Fig. 8. Moreover, compared with the SMF transmission systems FMF design proposed here have significantly higher effective area and have the advantage of multiple modes to increase the transmission capacity.

Table 1. Summary of the effective index differences between LP_{01}, LP_{11}, LP_{21} and LP_{02} modes and their effective areas after the introduction of air-holes in the proposed fiber designs.

Fiber Design	200 air-holes radius (nm)	Effective index difference (Δn_{eff})						Effective area (um^2)			
		S_1	$\%S_1$	S_2	$\%S_2$	S_3	$\%S_3$	LP_{01}	LP_{11}	LP_{21}	LP_{02}
Four mode fiber	55	0.002902017	29	0.003634979	28	0.00103236	26	97.57	136.36	154.53	136
Five mode fiber	70	0.002387145	30	0.003041579	29	0.00102063	38	118.85	162.55	171.57	101.09

4. Bending effect

Further simulations are carried out to study the effect of bending in our proposed FMF and compare that with a standard SMF. Higher order modes of a FMF are more resilient to bend distortion because they have larger effective index difference as compared to a fundamental mode for a given fiber. Moreover, effective area reduction of the fundamental mode is significantly larger compared to other higher order modes of a FMF [4, 20]. Hence, the bending loss and area reduction of only the fundamental mode in our proposed FMF is compared with a standard SMF. In order to compare these results, we considered a SMF with core radius 4.1 μm and cladding radius 35 μm. The refractive indices of core and cladding are taken as 1.44905 and 1.444, respectively.

Figure 9 shows variations of the bending loss with the bending radius (R_{bend}) for a standard SMF with a blue line. The bending losses of a five-mode fiber without air-holes and with air-holes are also shown in Fig. 9 by black and red lines, respectively. The bending loss of SMF at a R_{bend} of 5 mm is calculated as 9.97 dB/m and it increases as the bending radius is decreased. At $R_{bend} = 1$ mm, the bending loss of SMF has increased to a significantly higher value and calculated as 57.97 dB/m. However, the bending loss of a five-mode fiber (without holes) at 5 mm and 1 mm are calculated as 7.28×10^{-7} dB/m and 7.72 dB/m, respectively. This shows a significant reduction in the bending loss using a FMF compared to a standard SMF. Moreover, after introducing an array of 200 air-holes in our proposed FMF design, the bending loss reduces even further as shown by a red line in Fig. 9. At $R_{bend} = 1$ mm, the bending loss of five-mode fiber with air-holes is calculated as 3.59 dB/m which is nearly half of the value that was calculated without any air-holes.

Figure 10 shows the effect of bending on the effective area of a SMF and the fundamental mode of the FMF with and without air-holes. Due to the smaller core radius (4.1 μm), the effective area is calculated to be 78 μm^2 without any bending. This value is comparatively lower than

OSA CONTINUUM

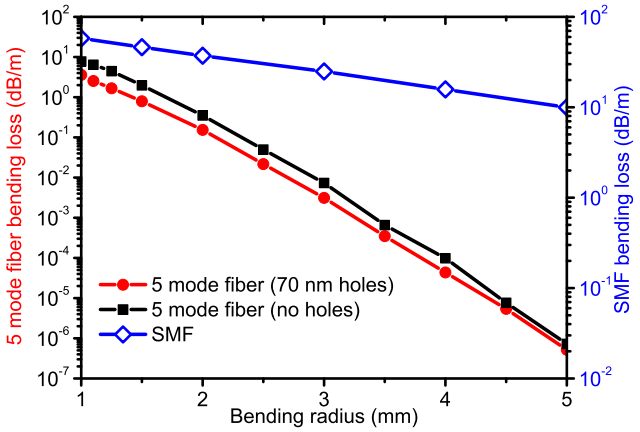

Fig. 9. Bending loss of a few-mode fiber without air-holes and with 200 air-holes with different bending radii. The bending loss of our proposed fiber is also shown by red line.

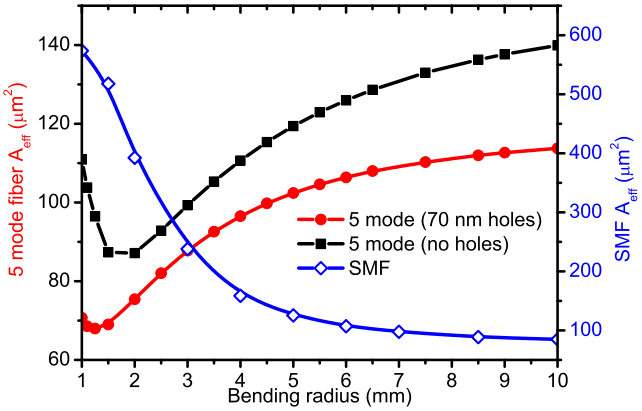

Fig. 10. Effective area as a function of bending radius for FMF without holes, with holes and a standard SMF.

the FMF with five modes, which is calculated as 151.92 μm^2 without any bending. Moreover, when the bending is introduced in SMF, the only guided mode quickly approaches to its cutoff value and the A_{eff} start increasing and calculated as 84.81 μm^2 at $R_{bend} = 10\ mm$. As shown by a blue line in Fig. 10, the A_{eff} of SMF continue to increase as the bending radius is further decreased to 1 mm and calculated as 573.67 μm^2.

However, compared to the SMF, the A_{eff} of a FMF (no holes) reduces with the decrease in R_{bend} and calculated as 139.92 μm^2 at $R_{bend} = 10\ mm$ as shown by a black line in Fig. 10. When the R_{bend} approaches to 2 mm, the A_{eff} of FMF (no holes) approaches to its cutoff and with further decrease in R_{bend}, the effective area start increasing. At $R_{bend} = 1\ mm$, the A_{eff} increases to 110.94 μm^2. Similar trend is observed in our proposed FMF (70 nm holes) design where, the A_{eff} is calculated as 113.76 μm^2 at $R_{bend} = 10\ mm$ and it further reduces as the R_{bend} is decreased. As shown by the red line in Fig. 10, the FMF with holes also approaches to its cutoff value at $R_{bend} = 1.25\ mm$ where the A_{eff} is calculated as 67.98 μm^2.

This shows that our proposed FMF design with the air-holes suffers from significantly less bending loss and also provides more stable modal operation compared to a conventional SMF or a standard FMF.

OSA CONTINUUM

5. Conclusion

We have proposed a new few-mode fiber design technique that is used to increase the modal spacing or effective index difference between the different modes of propagation. FMFs not only provides significantly larger effective areas but they are also capable of transmitting more optical power and can result in longer communication lengths. Our proposed technique involves the use of uniform air-holes array along the radius of the fiber such that the effective indices of the modes are decreased depending on their field profile at that particular location. We have shown that for a four-mode fiber design the modal stability between the modes can be increased more than 26% without a significant reduction in the mode quality. Moreover, we have also proposed another technique where a five-mode fiber is reduced to four modes and results in even higher (above 30%) effective index difference and also larger mode area compared to the first design. It is also shown here that the bending loss of FMFs with air-holes is significantly smaller and modal area is more stable with the bending. Such a fiber with air-holes can be fabricated, similar as a photonic crystal fiber. However, if needed the number of air-holes and their diameter can be adjusted to facilitate fabrication technique being considered.

References

1. R. J. Essiambre, G. Kramer, P. J. Winzer, G. J. Foschini and B. Goebel, "Capacity limits of optical fiber networks," J. Light. Technol. **28**(4), 662–701 (2010).
2. M. Secondini and E. Forestieri, "Scope and Limitations of the Nonlinear Shannon Limit," J. Light. Technol. **35**(4), 893–902 (2017).
3. B. Franz, and H. Bulow, "Mode group division multiplexing in graded–index multimode fibers," Bell Labs Tech. J. **18**(3), 153–172 (2013).
4. J. M. Fini, and S. Ramachandran, "Natural bend-distortion immunity of higher-order-mode large-mode-area fibers," Opt. Lett. **32**(7), 748–750 (2007).
5. A. Argyros, R. Lwin, and M. C. J. Large, "Bend loss in highly multimode fibres," Opt. Express **16**(23), 18590–18598 (2008).
6. S. Ramachandran, J. M. Fini, M. Mermelstein, J. W. Nicholson, S. Ghalmi, and M. F. Yan, "Ultra-large effective-area, higher-order mode fibers: a new strategy for high-power lasers," Laser Photon. Rev. **2**(6), 429–448 (2008).
7. R. Maruyama, N. Kuwaki, S. Matsuo and M. Ohashi, "Relationship between mode-crosstalk and fiber characteristics in few mode fibers," Optical Fiber Communications Conference and Exhibition (OFC), Anaheim, CA (2016), pp. 1–3.
8. F. Yaman, E. Mateo, and T. Wang, "Impact of modal crosstalk and multi-path interference on few-mode fiber transmission," Optical Fiber Communication Conference (OFC) (2012), paper OTu1D.2.
9. R. Ryf, S. Randel, A. H. Gnauck, C. Bolle, A. Sierra, S. Mumtaz, M. Esmaeelpour, E. C. Burrows, R. J. Essiambre, P. J. Winzer, and D. W. Peckham, "Mode-Division Multiplexing over 96 km of few-mode fiber using coherent 6×6 MIMO processing," J. Light. Technol. **30**(4), 521–531 (2012).
10. Y. Kokubun, T. Watanabe, S. Miura, and R.Kawata, "What is a mode in few mode fibers?: Proposal of MIMO-free mode division multiplexing using true eigenmodes," IEICE Electronics Express **13**(18), (2016).
11. T. Mori, T. Sakamoto, M. Wada, T. Yamamoto, and F. Yamamoto, "Few-Mode fibers supporting more than two LP modes for Mode-Division-Multiplexed transmission with MIMO DSP," J. Light. Technol. **32**(14), 2468–2479 (2014).
12. A. Gulistan, S. Ghosh, S. Ramachandran, and B. M. A. Rahman, "Efficient strategy to increase higher order inter-modal stability of a step index multimode fiber," Opt. Express **25**(24), 29714–29723 (2017).
13. J. Liang, Q. Mo, S. Fu, M. Tang, P. Shum, and D. Liu, "Design and fabrication of elliptical-core few-mode fiber for MIMO-less data transmission," Opt. Lett. **41**(13), 3058–3061 (2016).
14. R. A. May, and M. N. Zervas, "Few-mode fibers with improved mode spacing," IEEE Optical Communication (ECOC) (2015), pp. 1–3.
15. C. M. Rollinson, S. T. Huntington, B. C. Gibson, S. Rubanov, and J. Canning, "Characterization of nanoscale features in tapered fractal and photonic crystal fibers," Opt. Express **19**(3), 1860–1865 (2011).
16. Y. Ruan, H. Ebendorff-Heidepriem, S. Afshar, and T. M. Monro, "Light confinement within nanoholes in nanostructured optical fibers," Opt. Express **18**(25), 26018–26026 (2010).
17. P. Sillard, M. Astruc, D. Boivin, H. Maerten, and L. Provost, "Few-Mode Fiber for uncoupled Mode-Division Multiplexing transmissions," 37th European Conference and Exposition on Optical Communications, OSA Technical Digest (CD) Tu.5.LeCervin.7 (2011).
18. S. Virally, N. Godbout, S. Lacroix, and L. Labonte, "Two-fold symmetric geometries for tailored phasematching in birefringent solid-core air-silica microstructured fibers," Opt. Express **18**(10), 10731–10741 (2010).
19. M. J. Li, X. Chen, A. Liu, S. Gray, J. Wang, D. T. Walton, and L. A. Zenteno, "Limit of effective area for single-mode operation in step-index large mode area laser fibers," J. Light. Technol. **27**(15), 3010–3016 (2009).

OSA CONTINUUM

20. J. W. Nicholson, J. M. Fini, A. D. Yablon, P. S. Westbrook, K. Feder, and C. Headley, "Demonstration of bend-induced nonlinearities in large-mode-area fibers," Opt. Lett. **32**(17), 2562–2564 (2007).